Experimental Study of a Low-Modulus Flutter Strut for a Hydrofoil System

T. T. HUANG*
HYDRONAUTICS Inc., Laurel, Md.

The results of an experimental investigation of three low-modulus built-up struts with several rigid pods and foil configurations are presented. The scaled model struts were constructed using a copper alloy spine coated with an extremely low-modulus silicone rubber. The model was designed to reduce the model flutter speed to about $\frac{1}{4}$ that of the prototype. The test results for the low-modulus strut are in good agreement with scaled values from the prototype. In addition, a series of flutter tests were conducted to study the effects of strut sweep angle, strut submergence, pod weight, and foil angle of attack and dihedral on the flutter characteristics of the strut. The developed modeling technique may reliably be used to solve the practical hydrodynamic flutter problems and may serve as a guide for the future development of a useful theory which is presently unavailable.

I. Introduction

IN the past few years, the field of hydroelasticity has attracted a great deal of interest. Investigations of hydrofoil and strut flutter have been at the core of this interest because of its fundamental importance in the success of hydrofoil craft. The phenomenon of aircraft wing flutter is now rather well understood and satisfactory techniques for its prediction do exist. Unfortunately, these same techniques are not usable for the prediction of hydrodynamic flutter phenomena. The difficulty arises from the considerably larger density of the fluid surrounding hydrofoils compared to that surrounding aircraft wings. For aircraft wings, the mass of the surround fluid is almost inconsequential compared to the wind mass. This is not true for hydrofoils and, in fact, the added mass caused by the water surrounding a hydrofoil is usually larger than the mass of the hydrofoil. Classical flutter theory predicts that for ratios of foil mass to added mass below a certain value $\mu_{crit.}$ flutter is not possible. However, several occurrences of flutter have been systematically observed in tests of struts with mass ratios considerably below $\mu_{crit.}$[1,2] It is clear that the classical theory is inadequate. If a satisfactory technique is to be developed to predict this catastrophic phenomenon, it is crucial that experimental and theoretical investigations be conducted to observe and describe the physics of low mass ratio flutter.

Considerable progress has been made in the understanding of some facets of the hydrodynamic flutter phenomenon. Herr[3] has shown that the assumption of zero fluid damping eliminates the μ_{crit} asymptote at low mass ratios. However, this assumption has only a minor effect on the flutter boundary at the high mass ratios usually studied in aircraft flutter. The overestimation of the over-all damping ratio by the classical theory has been measured by experiments conducted by Henry.[4] In an attempt to correlate the flutter speed observed by Ransleben and Abramson[5] with theoretical flutter calculation, Abramson and Langner[6] arbitrarily shifted the phase angle of the Theodorsen function in their computation. Their results indicate that a phase shift of approximately 30° is required in order to predict the flutter speed. It appears that the unsteady aerodynamic force, which is derived on the basis of the ideal fluid assumptions, may not be sufficiently accurate for flutter analysis in the range of low mass density ratios typical of hydrofoil operation.

On the other hand, Baird et al.[7,8] have shown that prediction of strut flutter is very dependent on the number of modes used in the analysis. This study was somewhat inconclusive since increasing the number of assumed modes first improved the agreement with experimental results and then weakened the comparison. Baird's computations indicated that increasing the number of modes considered, that is, within the limitation of this study, resulted in monotonically decreasing flutter speeds. In his study, the assumed modes were those measured for the strut in air. The in-water modes were calculated from the measured in-air modes and the assumed added mass. It is known[9] that the in-water modes are significantly different from the in-air modes, and Baird's approach to the in-water modes or use of hydrodynamic strip theory may not be satisfactory. In addition, Dugundji and Ghareeb[10] found that the mode shapes at flutter change from a standing wave-type flutter at high mass ratio μ to a traveling wave type at low μ. Thus, modal analysis may not be feasible for the prediction of flutter at low μ.

One exceptionally important phenomenon is the flutter of strut-pod-foil systems typical of modern hydrofoil craft. It is fair to say that neither the prediction of flutter nor the flutter modeling of such systems is well developed. Mitchell and Rauch[11] discovered several surprising effects during the testing of the strut-pod-foil systems used on the FRESH I. For instance, increasing foil angle of attack was stabilizing in the case of the main foil system and destabilizing for the tail foil system. This result was unanticipated since the geometries of these systems were very similar. The analytical predictions for flutter of the tail struct proved conservative but those of the main strut failed to predict an important flutter mode. Because of the extreme complexity of the geometries and suspensions of the strut-pod-foil system involved in these tests, it does not seem possible to draw any conclusion from these results.

The means of determining the conditions for flutter and divergence instabilities is essential in the design of a hydrofoil craft. In light of the current inadequacy of prediction techniques, this can be accomplished only by tests on properly scaled models. Furthermore, it is important that the cost

Presented as Paper 68-125 at the AIAA 6th Aerospace Science Meeting, New York, January 22–24, 1968; submitted January 22, 1968; revision received April 22, 1968. This research was carried out under U.S. Naval Ship Systems Command General Hydromechanic Research Program, administered by Naval Ship Research and Development Center. The author expresses his sincere appreciation for the supervision and guidance received from W. C. Webster, E. Johnson Jr., and M. Martin of HYDRONAUTICS Inc.

* Associate Research Scientist; now Naval Architect (Hydromechanics), Naval Ship Research and Development Center, Washington, D. C. Associate Member AIAA.

in time and funds of such model construction be small enough so that design variation can readily be made when necessary.

Since October 1963, HYDRONAUTICS Inc. has been engaged in the development and testing of scaled low-modulus flutter models. Because of the complexity of the problem, the effort has been limited to the construction of low-modulus models of the struts tested by Baird et al.[7] The models were designed to reduce their flutter speeds to about $\frac{1}{4}$ that of the prototype.

The material developed in the first phase of this work has been reported by Ho.[12] His models were constructed of a mixture of polyester resin and styrene. Powdered tungsten carbide and glass fiber were added to the mixture to adjust the density and to reduce creep, respectively. These models stimulating the solid aluminum and solid steel struts were constructed and tested. The results of these flutter tests[12] are in good agreement with the results of Baird's struts.[7] However, this material has creep, fatigue, and aging shortcomings. It may not be suitable for modeling the strut-pod-foil system which is designed to carry a steady load. To overcome these defects a built-up strut was constructed of a copper alloy core embedded in an extremely low-modulus silicone compound coating to simulate Baird's base vented aluminum strut.[7] These models had negligible creep and internal damping. Flutter test in the HYDRONAUTICS channel at various depths and sweep angle showed good agreement with Baird's results. The tests were then extended to cover the investigation of the effects of a rigid pod alone and a rigid pod and foil combined on flutter characteristics of the strut.

II. The Models

The model consists of a low-modulus strut and rigid pod and fully wetted foils. The configuration was designed to be hydrodynamically similar to the E foil configuration[13] currently under consideration for the PGH by Code 6363, NAVSEC (formerly Code 420, Bureau of Ships). The specific features of these components are

1) The low-modulus built-up strut was constructed of a copper alloy coated with an extremely low-modulus silicone rubber. The strut nose was coated with plastic to avoid leading edge flutter, but the plastic was slit so as to eliminate any stiffness arising from the coating. The built-up strut has the same external configuration as Baird's no. 3 aluminum strut. The spite and coating were designed so that the values of the nondimensional constants such as the location of elastic axis and the center of gravity, the nondimensional torsion and bending moduli, the mass density, and the ratio of torsional stiffness to bending were equivalent to the full-scale configuration. Dimensions of the built-up struts have been constructed; one, with 15° sweep, was used to test the flutter characteristics of the strut alone. The others, with 0° and 20° sweep, were used to study the effects of the pod and foil on the strut flutter. The $\frac{1}{4}$ scale built-up model strut is shown in Fig. 1.

x	y
0	0
0.1"	0.020"
0.2"	0.030"
0.3"	0.032"
0.4"	0.034"
0.5"	0.036"
0.6"	0.038"
0.7"	0.040"
0.8"	0.042"
0.9"	0.044"
1.0"	0.046"
1.1"	0.048"
1.2"	0.050"
1.3"	0.052"
1.4"	0.053"
1.5"	0.054"
3.0"	0.054"

EXTERNAL ORDINATES

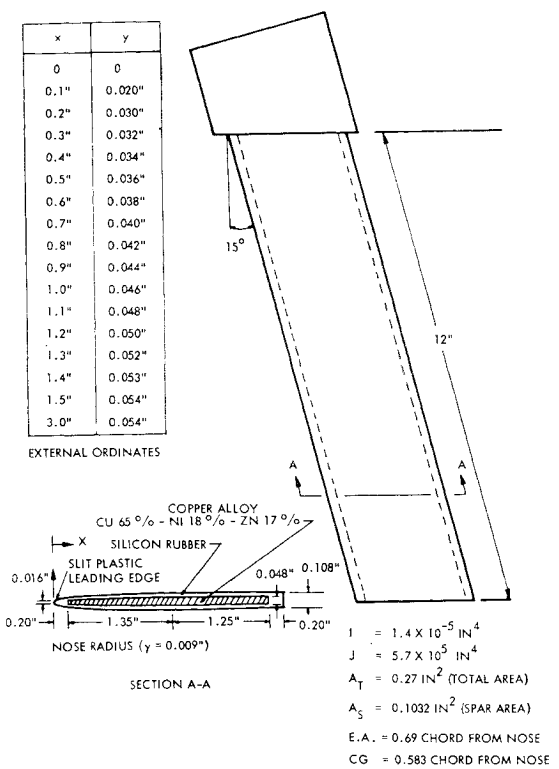

Fig. 1 $\frac{1}{4}$ scale built-up model strut.

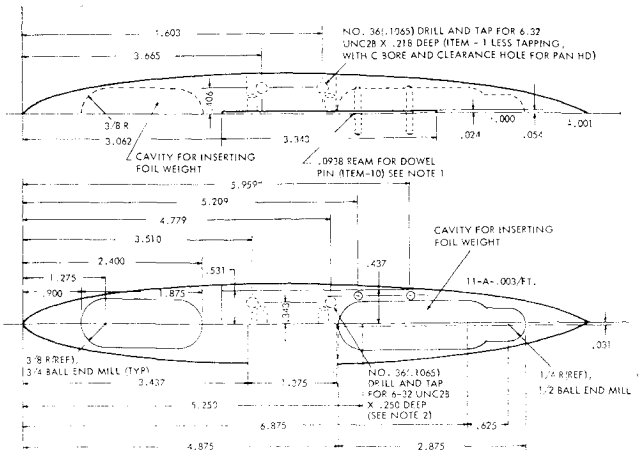

Fig. 2 Details of the pod.

2) The pod was a rigid series-58 body of revolution with the length of 8.74 in. The pod was connected to the tip of the low-modulus strut. The pod was constructed with internal cavities so that a foil weight could be inserted. The resultant pod weight system then has the same mass and yaw and inertial properties as the pod-foil system. The pod's center of gravity was located at the c.g. axis of the strut. Details of the pod are shown in Fig. 2.

3) The foil was a rigid, untapered section, hydrodynamically equivalent to the E foil (identical lift force slope and aerodynamic centerline). Variations of foil angle of attack and dihedral could be made during the test. The ordinates and the properties of the pod and foil are given in Fig. 3. Photographs of strut-pod-foil combinations are shown in Figs. 4–6.

III. Model Test Procedure

The flutter tests were conducted in the high-speed water channel at HYDRONAUTICS Inc. The model was attached rigidly to the supporting structure through a sway-force block gage. The gage was used for determining flutter frequency. A view of the model and its supporting system in the channel is shown in Fig. 7. The model was placed in the channel test section, and the speed of the water in the channel was increased gradually until flutter took place. The low-modulus strut was initially aligned with the direction of flow so that it had no side force until it began to flutter. The side force sensed by the block gage was recorded by a Honeywell visicorder. From the visicorder trace, one can determine the frequency of flutter when it occurs. The velocity at which flutter occurred was obtained from the manometer of the channel. Motion pictures were taken from the side and the bottom of the channel during the flutter.

The 15° swept low-modulus strut was tested at 10, 9, 8, and 6 in. of submergence out of the 12-in. total length. The sweep angle was varied from 10° to 25° at 5° increments for each depth of submergence. This test was conducted to study the

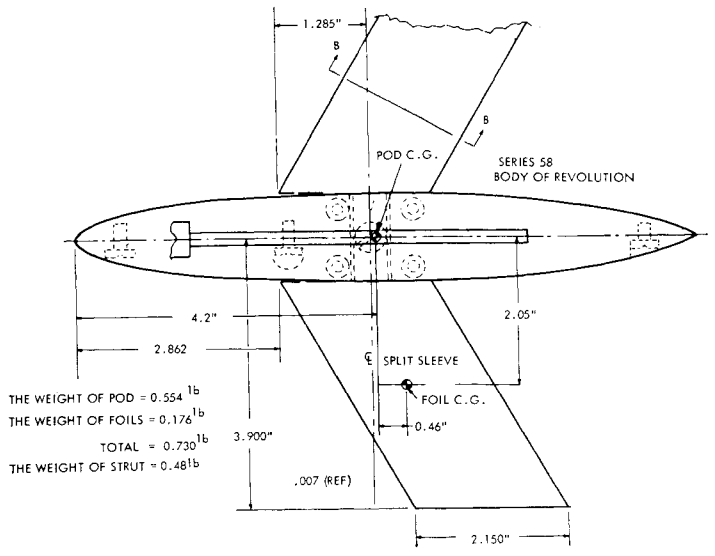

a)

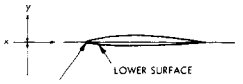

"18" - "18" NACA - (93175) 0.8 FOIL

UPPER SURFACE		LOWER SURFACE	
x	y	x	y
0.0000	0.0000	0.0000	0.0000
0.029	0.019	0.025	0.013
0.044	0.028	0.049	0.017
0.091	0.040	0.095	0.022
0.137	0.050	0.142	0.025
0.184	0.058	0.189	0.028
0.277	0.071	0.282	0.031
0.371	0.081	0.374	0.034
0.557	0.096	0.560	0.039
0.744	0.104	0.746	0.041
0.931	0.107	0.931	0.042
1.116	0.104	1.118	0.041
1.302	0.094	1.304	0.037
1.488	0.076	1.491	0.028
1.674	0.047	1.677	0.016
1.768	0.027	1.769	0.008
1.862	0.0000	1.862	0.0000

STATION	DISTANCE FROM NOSE	SERIES 58 RADIUS
0	0	.000
1/2	.437	.283
1	.874	.390
2	1.75	.520
3	2.62	.584
4	3.50	.616
5	4.37	.626
6	5.25	.607
7	6.12	.558
8	7.00	.464
9	7.87	.299
9 1/2	8.3	.183
10	8.74	.000

NOSE RADIUS .0893
TAIL RADIUS .0180

b)

Fig. 3 The pod and wing.

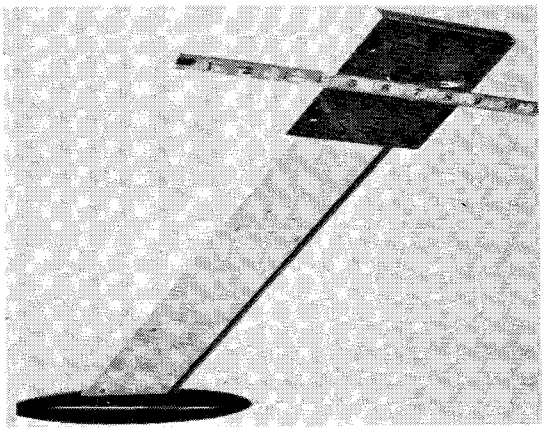

Fig. 4 The 20° low swept pod.

effects of sweep and submergence depth on the single strut. The results were used to compare the results of Ho's[12] strut and Baird's[7] strut in order to determine the merit of the built-up strut. The results are shown in Table 1 and Figs. 8 and 9.

The 20° swept model strut was tested to study the effects of various pod and foil configurarions on the flutter characteristics of the low-modulus strut. The strut and pod with and without foil weight at the depth of submergence varying from 6 to 10 in. was first tested. The strut and pod and foil at +2°, 0°, −2°, and −4° angles of attack was then tested at a similar range of depths. The results of these tests are given in Table 2 and Figs. 10 and 11. Finally, the strut submergence depth was kept at 10 in., three dihedral angles of the foil, 0°, +2°, and +4°, were used, and for each dihedral the foil angle of attack was varied from +6° to −6° at 1° increments. These results are shown in Table 3 and Figs. 12 and 13. In all tests, the strut was base vented, but cavitation free. No surface wave was observed during the test.

Further, the natural frequencies of both bending and torsion modes of the various configurations were measured in air. It was observed that the decays of oscillation amplitudes for all the modes tested in air were extremely small; thus, the structural damping may be regarded as negligibly small. These results, as well as the weights of the components, are given in Table 4.

IV. Results and Discussion

The predicted flutter velocity $V_{F(\text{predicted})}$ in Table 1 was obtained from Baird's experimental results[7] scaled to the

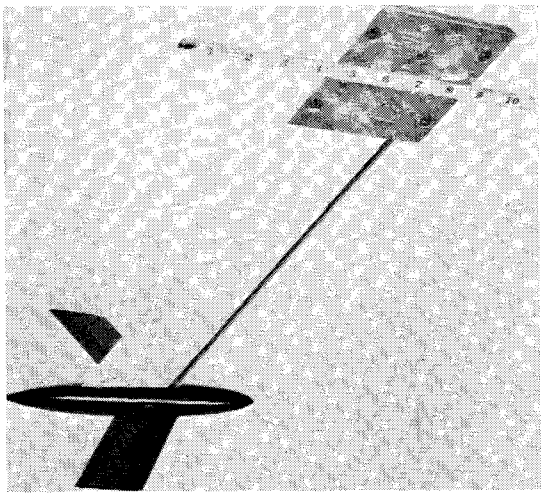

Fig. 5 Photograph of the 20° low-modulus strut with rigid pod and wing.

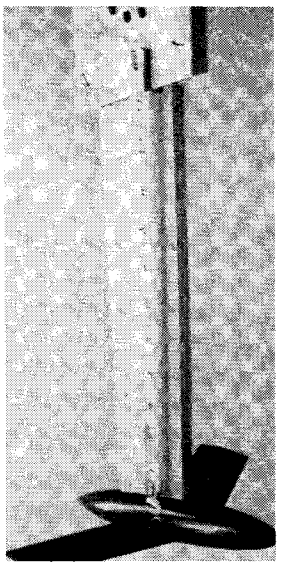

Fig. 6 Photograph of the vertical low-modulus strut with rigid pod and wing.

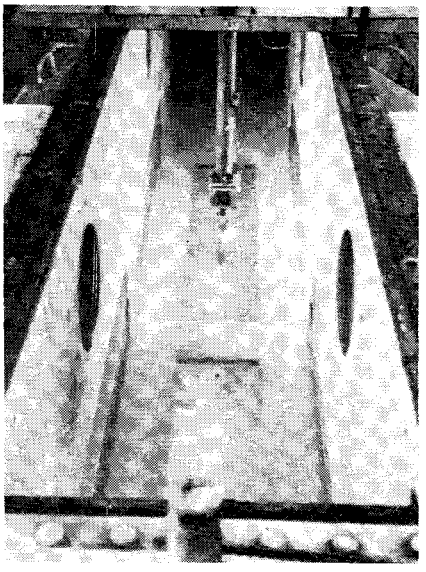

Fig. 7 A view of the model and its supporting system.

model tested by

$$V_{F(\text{predicted})} = V_{F(\text{prototype})} \times \left\{ \frac{(EI)_{\text{model}}}{(EI)_{\text{prototype}}} \right\}^{1/2} \times \left\{ \frac{A_{\text{prototype}}}{A_{\text{model}}} \right\}$$

where EI is the bending stiffness and A the cross-section area. $(EI)_{\text{model}}$ of the built-up strut obtained from the deflection measurement is 572 lb-in.^{2}. $(EI)_{\text{prototype}}$ given in Ref. 7 is 4.46×10^5 lb-in.^{2} The ratios of EI to GJ for model and prototype were all equal to 1.6. The value of $(A_{\text{prototype}}/A_{\text{model}})$ here is 15.2. The flutter frequency was predicted using

$$\frac{f_{\text{prototype}}}{f_{\text{model}}} = \frac{V_{F(\text{model})}}{V_{F(\text{prototype})}} \frac{L_{(\text{prototype})}}{L_{(\text{model})}}$$

where f is the flutter frequency and L is a typical dimension of the struts. The measured flutter velocities shown in Table 1 agree with the predicted values within 10% (the measured values are on the conservative side). The measured flutter frequencies are in good agreement with the scaled values from the prototype. It is important to note that, although the strut flutters at 11° sweep, a large divergence occasionally occurs during flutter. Thus, the strut appears to be close to the intersection of flutter and divergence boundaries at 10° sweep. The flutter was more readily obtained in the present test than that in the prototype since the present test was conducted in a stationary channel rather than a towing tank which can only provide a very short range of constant test speed.

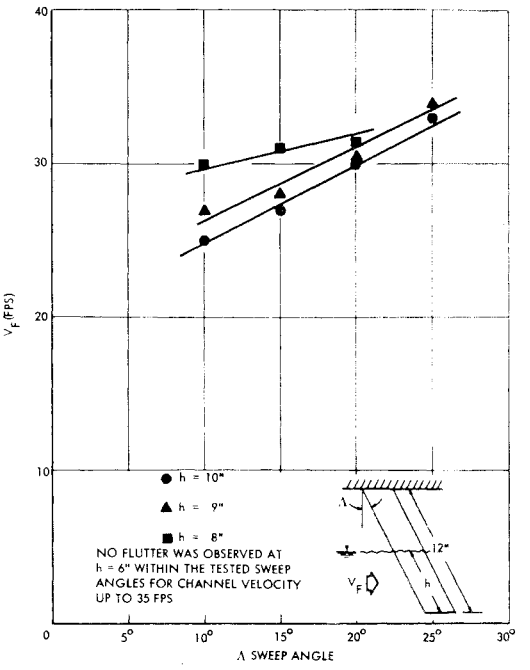

Fig. 8 Flutter velocities of the low-modulus strut at various sweeps and submergences.

Since the built-up strut does not have creep, fatigue, and aging limitation, the structure is so strong that failure never occurred even after severe flutter and divergence. The experimental data were repeatable and were in reasonable agreement with the scaled values from the prototype. Thus, it was decided to use the built-up strut in the flutter study of the strut-pod-foil configuration.

As shown in Fig. 8, the strut-flutter velocity increases with the increase of sweep angle for each depth of submergence, and for a given sweep the flutter velocity of the strut alone decreases with increasing submergence (see Fig. 10). These

Table 1 Predicted and measured flutter velocities and frequencies of the built-up and the plastic model struts

		Built-up strut				Plastic strut[g]			
		Flutter velocity V_F, fps		Flutter frequency f, cps		Flutter velocity V_F, fps		Flutter frequency f, cps	
Angle of sweep, deg	Depth of submergence, in.	Pred.[a] flutter	Meas. flutter	Pred.[a]	Meas.	Pred.[a] flutter	Meas. flutter	Pred.[a]	Meas.
25	10	40	33.0	6.25	6.0	27.5	27.0	4.3	4.4
25	9	...	34.0	...	6.2	...	...	...	...
25	8	...	none up to 35.0	...	...	...	...	...	...
25	6	...	none up to 35.0	...	...	...	...	...	...
20	10	33	30.0	4.35	4.6	22.0	22.5	2.9	3.0
20	9	34	30.5	4.35	4.8	23.1	24.0	2.9	2.8
20	8	...	31.5	...	4.9	...	...	...	...
20	6	...	none up to 35.0	...	...	...	...	...	...
15	10	29.2	27	3.34	3.3	22	22	3.3	3.0
15	9	...	28	...	3.5	...	...	...	...
15	8	...	31	...	3.7	...	...	...	...
15	6	...	none up to 35.0	...	...	...	...	...	...
10	10	26.8	25	2.32	2.0	18.0	18.7	1.5	1.6
10	9	28	27	2.2	2.4	19.0	20.0	1.4	1.5
10	8	...	30	...	2.8	...	...	...	...
10	6	...	none up to 35.0	...	...	...	...	...	...

[a] Predicted flutter velocities and frequencies are calculated from Baird's measurements[7] scaled to models tested.

Table 2 Flutter test results of the 20° swept low-modulus strut with various pod and foil configurations

Depth of submergence, in.	Strut and pod without foil weight		Strut and pod with foil weight		Strut-pod-foil[a]			
					−2° angle of attack		−4° angle of attack	
	Flutter velocity V_F, fps	Flutter frequency f, cps	Flutter velocity V_F, fps	Flutter frequency f, cps	V_F, fps	f, cps	V_F, fps	f, cps
10	34	5.2	16.0	7.9	30.5	5.4	28.0	5.0
9	30	5.8	15.0	8.2	31.0	4.5	29.0	4.6
8	25.5	8.7	14.0	8.3	34.5	4.2	30.0	4.4
6	20	10.5	14.0	9.0	none up to 35.0	...	33.0	3.6

[a] No flutter for +2° and 0° angles of attack (0°: maximum speed tested, 32 fps; +2°: 26 fps begin to diverge).

Table 3 Flutter test results of the 20° swept low-modulus strut with pod and foil at various angles of attack and dihedral

Foil angle of attack, deg	Dihedral, angle of the θ = 0°		θ = 2°		θ = 4°	
	V_F, fps	f, cps	V_F, fps	f, cps	V_F, fps	f, cps
+6	none up to 32.0	...	slowly diverges at 33.0	...	slowly diverges at 32.0	...
+4	none up to 32.0	...	slowly diverges at 33.0	...	slowly diverges at 32.0	...
+3	none up to 32.0	...	none up to 33.0	...	slowly diverges at 32.0	...
+2	none up to 32.0	...	none up to 33.0	...	slowly diverges at 32.0	...
+1	none up to 32.0	...	none up to 33.0	...	slowly diverges at 32.0	...
0	none up to 32.0	...	none up to 33.0	...	slight flutter at 32.0	...
−1	none up to 32.0	...	31.0	6.0	32.2	6.4
−2	30.5	5.4	30.5	5.6	31.5	6.0
−3	29.0	5.2	29.0	5.2	30.0	5.6
−4	28.0	5.0	28.0	5.1	29.0	5.4
−5	26.5	4.9	27.0	5.1	27.5	5.3
−6	26.0	4.8	26.0	4.9	27.0	5.0

trends were also reported in the calculations by Herr[3] and by Squires.[15] It can be concluded that the theoretical trends of the effects of sweep and submergence on the flutter velocity of the strut alone are in good agreement with the present data.

The effects of the rigid pod and the rigid foil on the strut flutter characteristics are shown in Table 2 and Figs. 10 and 11. The data presented are for the strut at 20° sweep. For zero swept strut, the strut tends to diverge (at rather low

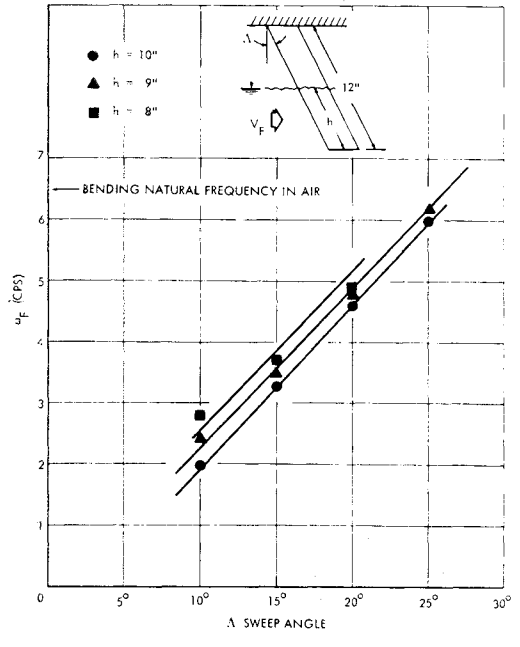

Fig. 9 Flutter frequencies of the low-modulus strut at various sweeps and submergences.

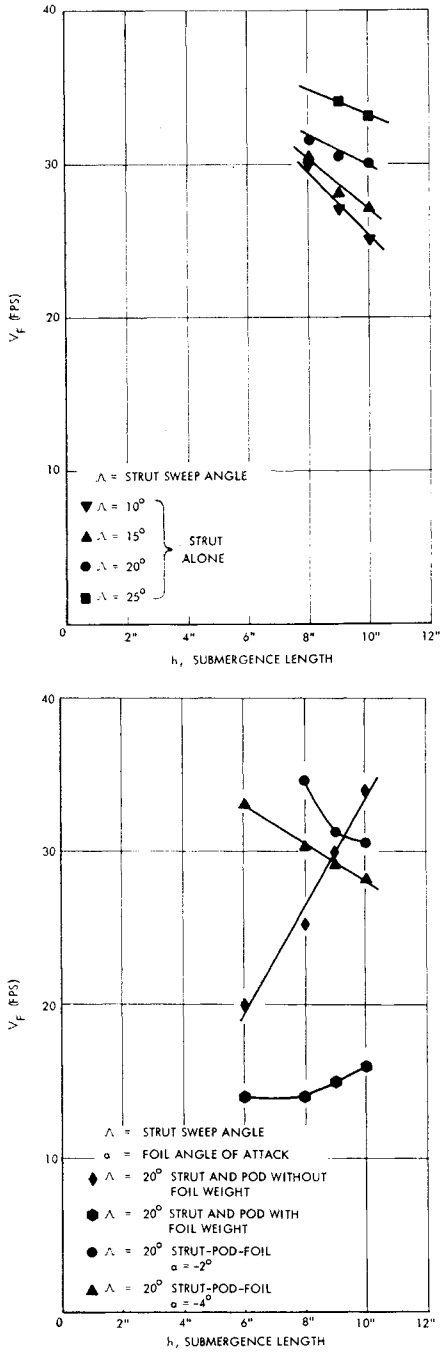

Fig. 10 Flutter velocities of the low-modulus strut with various pod and foil configuration.

Table 4 Weights of the components and the measured torsional and bending natural frequencies in air

I.	Weights of the components, lb
	a. Strut, 0.48 (root fixture excluded)
	b. Pod, 0.554
	c. Foil, 0.176
II.	Measured strut torsional natural frequencies in air, cps
	a. Strut and pod without foil weight, 16
	b. Strut and pod with foil weight, 12.8
	c. Strut and pod-foil, 12.8
III.	Measured strut bending natural frequencies in air, cps
	a. Strut and pod without foil weight, 3.3
	b. Strut and pod with foil weight, 2.9
	c. Strut-pod-foil, 2.9
	d. Strut alone, 6.5

speed, 15–20 fps) rather than flutter for all configurations shown in Table 2.

As shown in Fig. 10, the 20° swept strut and the pod fluttered at lower speeds with the foil weight than without the foil weight. Increasing the submergence only increases the flutter velocity of the strut and the pod with the foil weight slightly. However, the flutter velocity of the strut and the pod without foil weight increases rapidly with increasing submergence similar to the results by Squires,[15] who computed the flutter velocity of a typical strut-pod-foil configuration. The generalized mass density ratio of the strut and pod without foil weight may be in the neighborhood of its critical mass density ratio, and by adding the foil weight in the pod the generalized mass density ratio of the system may exceed its critical value by a considerable amount. The measured drastic change of flutter characteristics from the strut and pod without foil weight to that with weight is probably due

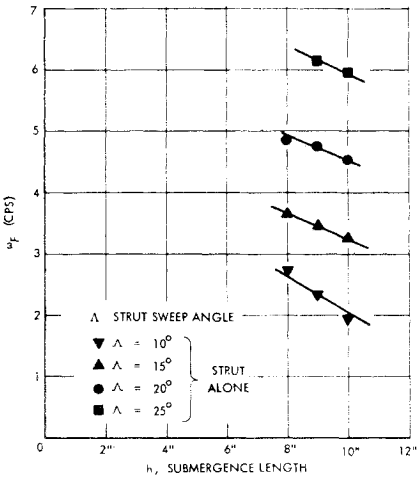

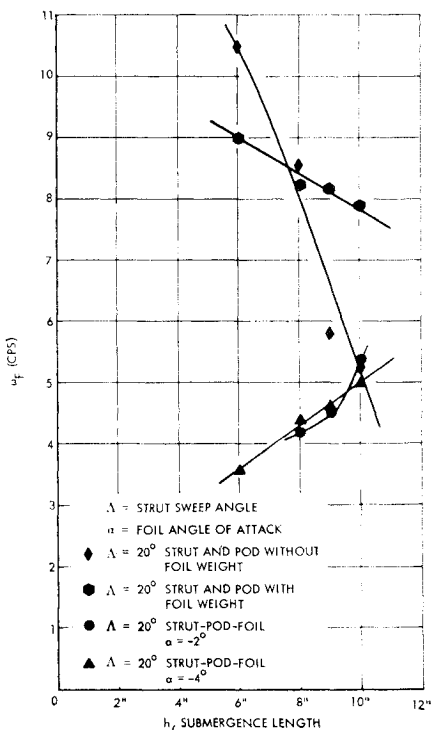

Fig. 11 Flutter frequencies of the low-modulus strut with various pod and foil configuration.

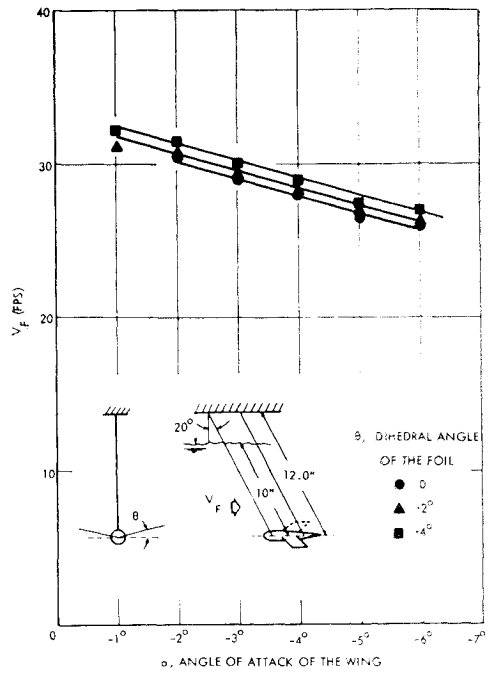

Fig. 12 Flutter velocities of the 20° swept low-modulus strut with pod and foil at various angles of attack and dihedral.

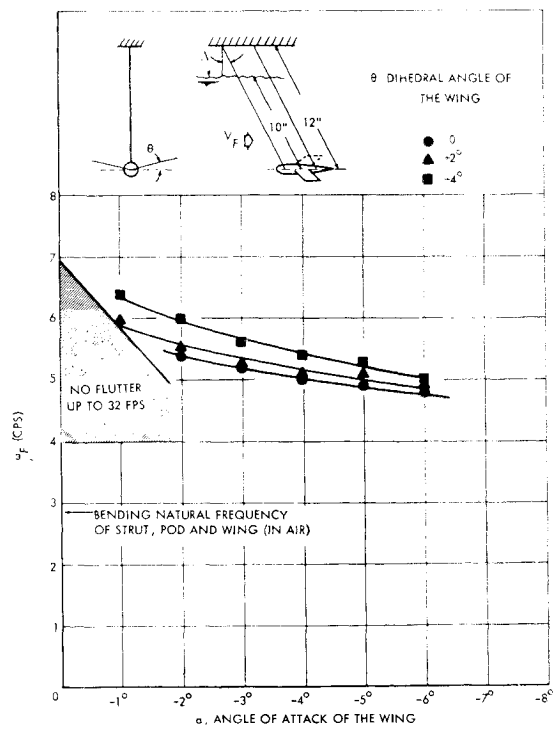

Fig. 13 Flutter frequencies of the 20° swept low-modulus strut with pod and foil at various angles of attack and dihedral.

to this effect (see Fig. 8 of Herr[3]). As shown in Fig. 11, the flutter frequencies for the strut and the pod with and without foil weight decrease with increasing submergence.

For the 20° swept strut-pod-foil, no flutter was observed with the foil at zero angle of attack up to 32 fps, but the strut began to diverge at about 26 fps when the foil was at +2° angle of attack. However, at −2° and −4° angles of attack the strut fluttered within the test range. The flutter velocity decreases but the flutter frequency increases with increasing submergence. It is important to note that, when the foil is at 0° angle of attack, the foil damping prevents the strut from fluttering within the test range, whereas strut and pod with and without foil weight all flutter within the test range. For the foil at positive angles of attack, the foil static loading tends to reduce the divergence speed in the present configuration. However, when the foil is at negative angles of attack, the foil static loading tends to increase the strut divergence speed but decrease the strut flutter velocity. The downward force caused by the foil at a negative angle of attack results in an apparent stiffening of the strut. This increase in apparent stiffness causes a higher strut natural frequency and produces the aforementioned phenomena.

From the analysis of the motion picture, it is observed that the flutter of the tested struts is continuous, regular, and of bending-torsion type with a few fundamental modes. Flutter of the strut alone is dominated by the first bending and torsion modes and the bending amplitude is considerably larger than the torsion amplitude. Flutter of the strut and pod both with and without foil weight is dominated by the second bending and the first torsion modes, and the torsion amplitude is larger than the bending amplitude. The torsion amplitude of the strut and pod is much larger, and its bending amplitude is much smaller than that of the strut alone. In the flutter of the strut-pod-foil system, the first and second bending and the first torsion modes can be identified. Sometimes the mode shape change from the second bending to the first bending was observed during the test. The bending and torsion amplitudes are equally large in the flutter of the strut-pod-foil system. In one or two cases the traveling wave modes appear to be present.

V. Conclusions

The developed low-modulus built-up flutter model offers an attractive technique for the study of hydroelasticity since it does not have creep, fatigue, or brittleness shortcomings, and the experimental data were repeatable and were in reasonable agreement with the scale values from the prototype.

The theoretical prediction of the flutter of the complete strut-pod-foil system is far from satisfactory. Thus, this reliable model technique is of fundamental importance for solving the immediate practical problem, whereas the existing theory is not yet dependable and may serve as a guide for future development of a useful theory. The flutter characteristics such as mode shape and frequency in the present test can be carefully observed. Such observation may be useful for the modal-type analysis.

Within the range of the present tests, the flutter velocity of the strut alone increased with increase of sweep angle and with decrease of submergence. The 20° swept strut and pod fluttered at lower speeds with the foil weight than without the foil weight. In the test of the strut-pod-foil system, no flutter was observed with the foil at zero angle of attack up to 32 fps. The strut began to diverge at about 26 fps when the foil was at +2° angle of attack. At −2° and −4° angles of attack the strut fluttered at velocities smaller than 35 fps.

References

[1] Woolston, D. S. and Castile, G. E., "Some Effects of Variations in Several Parameters Including Fluid Density on the Flutter Speed of Light Uniform Cantilever Wings," TN 2558, Dec. 1951, NACA.

[2] Hilborne, C. V., "The Hydro-elastic Stability of Hydrofoil Strut," R & M 3172, 1960, Aeronautical Research Council, Great Britain.

[3] Herr, R. W., "A Study of Flutter at Low Mass Ratios With Possible Application to Hydrofoils," TN D-831, May 1961, NACA.

[4] Henry, C. J., "Hydrofoil Flutter Phenomenon and Airfoil Flutter Theory," Rept. R-856, Sept. 1961, Davidson Lab.

[5] Ransleben, G. E., Jr. and Abramson, H. N., "Experimental Determination of Oscillatory Lift and Moment Distributions Fully Submerged Flexible Foils," *Journal of Ship Research*, Vol. 7, No. 2, Oct. 1963, pp. 24–41.

[6] Abramson, H. N. and Langner, C. G., "Correlation of Various Subcavitating Hydrofoil Flutter Predictions Using Modified Oscillatory Lift and Moment Coefficients," Report, Contract NObs-88599, June 1964, Southwest Research Institute.

[7] Baird, E. F., Squires, C. E., Jr., and Caporali, R. L., "An Experimental and Theoretical Investigation of Hydrofoil Flutter," Paper 62–55, Jan. 1962, IAS.

[8] Baird, E. F., Squires, C. E., Jr., and Caporali, R. L., "Investigation of Hydrofoil Flutter," Final Report, Rept. DA 10-480-3, Feb. 1962, Grumman Aircraft Engineering Corp.

[9] Peller, R. and Figueroa, L., "Experimental Investigation of Supercavitating Hydrofoil Flutter Phenomena," Rept. GDC-63-132A, Aug. 1963, General Dynamics/Convair.

[10] Dugundji, J. and Ghareeb, N., "Pure Bending Flutter of a Swept Wing in a High Density, Low Speed Flow," Fluid Dynamics Research Group Rept. 64-1, March 1964, Massachusetts Institute of Technology.

[11] Mitchell, L. and Rauch, F. J., Jr., "Dynamic Tests of the $\frac{1}{4}$ Scale Models of the 80 Knot Transiting Strut-Foil Systems for the Fresh I Hydrofoil Test Craft," Draft Report, Rept. DA M51-239, Aug. 1964, Grumman Aircraft Engineering Corp.

[12] Ho, H. W., "The Development and Testing of Low Modulus Flutter Models of a Base-Vented Strut," TR 495-1, May 1965, HYDRONAUTICS Inc.

[13] Curtis, E. C., "The Static Performance of a $\frac{1}{5}$ Scale Model of the BuShips E Foil Configuration," TR 507-2, Aug. 1965, HYDRONAUTICS Inc.

[14] Bisliplinghoff, R. L., Ashley, H., and Halfman, R. L., *Aeroelasticity*, Addison-Wesley, Reading, Mass., 1955.

[15] Squires, C. E., Jr., "Hydrofoil Flutter—Small Sweep Angle Investigation," Final Rept., Rept. DA Nonr 3989.3, Nov. 1963, Grumman Aircraft Engineering Corp.